J|A|C|S
COMMUNICATIONS

Published on Web 05/06/2004

Multistep Energy Transfer in Single Molecular Photonic Wires

Mike Heilemann,[†] Philip Tinnefeld,[†] Gabriel Sanchez Mosteiro,[‡] Maria Garcia Parajo,[‡] Niek F. Van Hulst,[‡] and Markus Sauer*,[†]

Applied Laserphysics & Laserspectroscopy, Physics Faculty, University of Bielefeld, Universitätsstrasse 25, 33615 Bielefeld, Germany, and Applied Optics Group, Department of Applied Physics and MESA+ Research Institute, University of Twente, P.O. Box 217, 7500 AE Enschede, The Netherlands

Received February 5, 2004; E-mail: sauer@physik.uni-bielefeld.de

A photonic wire is a molecular device that conveys excited-state energy from an input to an output unit.[1,2] In contrast to conductive nanowires, photonic wires are addressable at a distance without the need of physical contacts. In 1994, Lindsay and co-workers realized the first molecular photonic wire based on conjugated porphyrin arrays.[1] However, strongly coupling porphyrin arrays exhibit the disadvantage of forming so-called energy sinks due to different local interactions of the chromophores.[3] Furthermore, as molecular photonic wires have to operate at the single molecule level they have to be studied at this individual level as well. Therefore, the chromophores used have to exhibit special spectroscopic characteristics, such as high photostability and fluorescence quantum yield. The ideal photonic wire consists of a very regular arrangement of chromophores which allows for efficient energy transfer but prevents alterations of photophysical properties of the individual chromophores, resulting in the formation of energy sinks.

In this communication, we report on the development of a molecular photonic wire based on (i) the use of conventional chromophores with high fluorescence quantum yield, (ii) an energy cascade as the driving force for the excited-state energy to ensure unidirectionality, and (iii) an arrangement of the chromophores such that strong electronic interactions promoting fluorescence quenching are prevented. Because of the unique molecular recognition properties and the scaffoldlike structure, double-stranded DNA constitutes an ideally suited building block on which to base the construction of nanoscale molecular devices. In addition, the use of DNA offers many well-developed labeling and post-labeling strategies to introduce a variety of different chromophores in a modular conception, i.e., short oligonucleotides carrying the desired chromophores can be selectively hybridized to a complementary template strand (Figure 1). The resulting wire is addressed by excitation of the primary donor, which transfers excited-state energy according to Förster theory[4] by weak dipole−dipole induced chromophore interactions through the transmitter chromophores to the final acceptor. The acceptor releases the transferred energy by emission of a fluorescence photon.

To realize a unidirectional photonic wire based on multistep fluorescence resonance energy transfer, five different chromophores were attached covalently to single-stranded DNA fragments of various lengths (60 or 20 bases). Hybridization of the labeled DNA fragments results in a double-stranded 60 base pair (bp) DNA construct containing five chromophores at well-defined positions and distances. To ensure highly efficient fluorescence resonance energy transfer (FRET) without quenching electronic interactions, an interchromophore distance of 10 bp corresponding to 3.4 nm was used.[6] The overall spatial range covered by this photonic wire is 13.6 nm. The spectral range comprises more than 200 nm of the visible spectrum, starting from ∼488 to ∼700 nm. As calculated from the spectroscopic characteristics of singly labeled oligonucleotides, each FRET step should occur with ∼90% efficiency, assuming free rotation of the chromophores ($\kappa^2 = 2/3$).

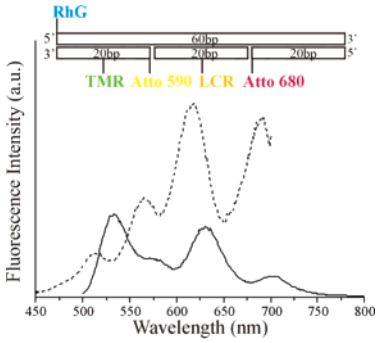

Figure 1. Fluorescence emission (488 nm excitation, straight line) and excitation spectrum (705 nm fluorescence, dotted line) of a DNA-based photonic wire containing five fluorophores measured in PBS, pH 7.4. The upper sketch demonstrates the synthesis strategy used to incorporate five different chromophores into double-stranded DNA at well-defined positions. TMR was introduced via phosphoramidite chemistry. All other chromophores were covalently attached to amino-modified oligonucleotides using standard NHS chemistry.

Calculation of the overall efficiency for energy transfer from the first donor Rhodamine Green (RhG) via tetramethylrhodamine (TMR), Atto 590, and LightCycler Red (LCR) to the final acceptor Atto 680 using the decrease in donor intensity or the relative intensities of the excitation spectrum (Figure 1) delivers strongly different values of ∼15 and ∼30%, respectively. However, it can be anticipated that because of the huge size and complexity of the system, unfavorable conformational orientations of the chromophores, insufficient hybridization, and/or additional quenching pathways including electron-transfer reactions with DNA nucleotides[7] will generate an inhomogeneous broadening of the transfer efficiency observed form ensemble measurements.

Therefore, we applied single molecule spectroscopy (SMS)[8] in combination with spectrally resolved confocal fluorescence scanning microscopy on four detectors using the 488 nm line of an argon ion laser for almost exclusive excitation of the first donor RhG. Sample molecules were randomly adsorbed on dried glass surface and scanned using a piezoelectric *x*,*y*-stage. Fluorescence photons were collected with the same objective and split onto four spectrally separated avalanche photodiodes (APDs) using dichroic beam splitters. The signal of the APDs was fed to a photon counting PC card for data storage and analysis. In the fluorescence image (Figure 2a), the detector channels are encoded in blue (503−548 nm), green (560−600 nm), yellow (600−680 nm), and red (680−738 nm).

As indicated by the four different colors in Figure 2a, the majority of fluorescence spots is dominated by the emission of one of the

[†] University of Bielefeld.
[‡] University of Twente.

10.1021/ja049351u CCC: $27.50

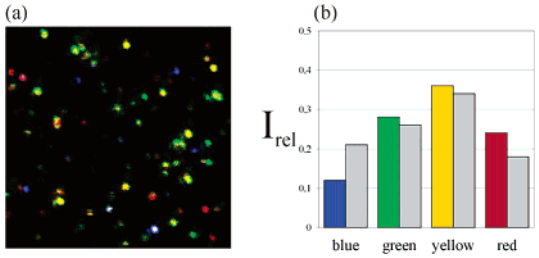

Figure 2. (a) False color fluorescence intensity image (10 × 10 μm) of photonic wires adsorbed on dry glass surface (488 nm excitation, 50 nm/pixel, 2 ms integration time, 10−100 counts/2 ms). The different colors demonstrate strongly different multistep FRET efficiencies. (b) Histogram of spectral characteristics of 200 photonic wires (color columns) compared to the distribution as expected (calculated) from the ensemble emission spectrum (gray columns).

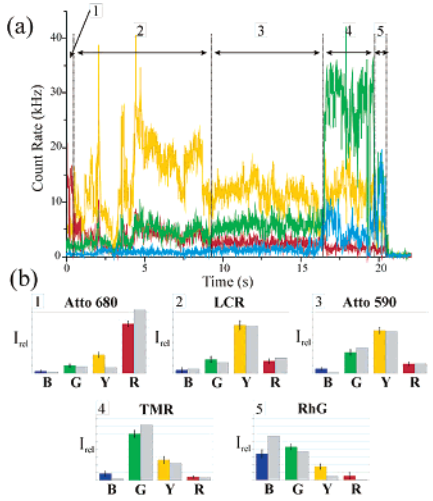

Figure 3. (a) Fluorescence intensity trajectory of an individual photonic wire measured on the four spectrally separated APDs (3 kW/cm^2 average excitation intensity at 488 nm). Five different emission patterns can be observed indicating that subsequent photobleaching of the chromophores starting with Atto 680 (part 1) occurred. (b) Intensity patterns (color columns) measured for the five different parts are compared to those (gray columns) measured for singly labeled oligonucleotides.

five chromophores. Besides unfavorable conformations and competing quenching pathways, premature photobleaching of chromophores can also substantially decrease the observed overall energy transfer efficiency. On the other hand, about 10% of all photonic wires show predominately emission on the red channel, that is, unidirectional highly efficient (∼90%) multistep energy transfer across 13.6 nm. With the exception of the blue channel, the histogram constructed from 200 individual fluorescence spots corresponds well to the ensemble fluorescence spectrum of the photonic wire (Figure 2b). The deviation found for the blue channel is a result of the lower photostability and a second red-shifted emissive state of the first donor RhG when immobilized on dry glass surface (see Supporting Information).

For further characterization of multistep FRET, single photonic wires were placed in the laser focus, and their fluorescence intensity was recorded until irreversible stepwise photobleaching occurred (Figure 3a). To attribute the emission pattern recorded on the four spectrally separated detection channels to a certain chromophore, the five chromophores were measured independently but under otherwise identical conditions, i.e., conjugated to DNA strands, to obtain chromophore specific detection patterns (gray columns in Figure 3b). According to these patterns, five regions with different spectral characteristics can be retrieved from the four different fluorescence intensity trajectories. The first 0.4 s of the trajectory (part 1) can be attributed to the emission of the far red chromophore Atto 680. After photobleaching of the final acceptor, the fluorescence emission is dominated by LCR (part 2) followed by Atto 590 (part 3), TMR (part 4), and finally RhG (part 5). Overall, five subsequent photobleaching events can be uncovered. Comparison of the intensity patterns measured (color columns) to the ones expected for the different chromophores (gray columns) demonstrates that the fluorescence emission is dominated by one chromophore at all times. Small deviations, e.g., those observed for part 1 in Figure 3b, indicate less efficient energy transfer between some chromophores, i.e., a leakage of the wire, possibly induced by unfavorable orientations of some chromophores.

For the first time, we demonstrate multistep FRET in a DNA-based unidirectional photonic wire carrying five spectrally different chromophores. SMS on four spectrally separated detectors demonstrates that individual photonic wires exhibit overall FRET efficiencies of up to ∼90% across a distance of 13.6 nm and a spectral range of ∼200 nm. The strength of the approach is the synthetic simplicity of the modular conception as well as the free choice of chromophores, which provides the basis for the investigation of photophysical pathways in molecular photonic devices even at the single molecular level. Currently, we are working on the development of a labeling strategy that enables accurately defined and rigid orientations of the chromophores and the insertion of a photoswitch[9] to enable the controlled switching of the photonic wire via a second independent laser line.

Acknowledgment. We gratefully acknowledge support of the VW-Stiftung (Grant I/78 094).

Supporting Information Available: Synthesis of the photonic wire, experimental details, and fluorescence images of RhG (PDF). This material is available free of charge via the Internet at http://pubs.acs.org.

References

(1) (a) Wagner, R. W.; Lindsey, J. S. *J. Am. Chem. Soc.* **1994**, *116*, 9759−9760.
(2) (a) Kawahara, S.; Uchimaru, T.; Murata, S. *Chem. Commun.* **1999**, 563−564. (b) Shchepinov, M. S.; Korshun, V. A. *Nucleosides, Nucleotides Nucleic Acids* **2001**, *20*, 369−374. (c) Ohya, Y.; Yabuki, K.; Hashimoto, M.; Nakajima, A.; Ouchi, T. *Bioconjugate Chem.* ***2003***, *14*, 1057−1066.
(3) Kim, Y. H.; Jeong, D. H.; Kim, D.; Jeoung, S. C.; Cho, H. S.; Kim, S. K.; Aratani, N.; Osuka, A. *J. Am. Chem. Soc.* **2001**, *123*, 76−86.
(4) Förster, T. *Discuss. Farraday Soc.* **1959**, *27*, 7−17.
(5) Bustamante, C.; Marko, J. F.; Siggia, E. D.; Smith, S. *Science* **1994**, *265*, 1599−1600.
(6) Dietrich, A.; Buschmann, V.; Müller, C.; Sauer, M. *Rev. Mol. Biotechnol.* **2002**, *82*, 211−231.
(7) (a) Heinlein, T.; Knemeyer, J. P.; Piestert, O.; Sauer, M. *J. Phys. Chem. B* **2003**, *107*, 7957−7964. (b) Piestert, O.; Barsch, H.; Buschmann, V.; Heinlein, T.; Weston, K. D.; Sauer, M. *Nano Lett.* **2003**, *3*, 979−982.
(8) (a) Ha, T.; Enderle, T.; Ogletree, D. F.; Chela, D. S.; Selvin, P. R.; Weiss, S. *Proc. Natl. Acad. Sci. U.S.A.* **1996**, *93*, 6264−6268. (b) Weiss, S. *Science* **1999**, *283*, 1676−1683. (c) Tinnefeld, P.; Herten, D.-P.; Sauer, M. *J. Phys. Chem. A* **2001**, *105*, 7989−8003.
(9) (a) Irie, M.; Fukaminato, T.; Sasaki, T.; Tamai, N.; Kawai, T. *Nature* **2002**, *420*, 759−760. (b) Terazono, Y.; Kodis, G.; Andréasson, J.; Jeong, G.; Brune, A.; Hartmann, T.; Dürr, H.; Moore, A. L.; Moore, T. A.; Gust, D. *J. Phys. Chem. B* **2004**, *108*, 1812−1814.

JA049351U